HHS Public Access

Author manuscript

Oncogene. Author manuscript; available in PMC 2019 July 18.

Published in final edited form as:

Oncogene. 2017 January 26; 36(4): 525–533. doi:10.1038/onc.2016.223.

Androgen Deprivation Leads to Increased Carbohydrate Metabolism and Hexokinase 2 Mediated Survival in *Pten/Tp53* Deficient Prostate Cancer

Philip L. Martin[1,#], **Juan-Juan Yin**[1], **Victoria Seng**[1], **Orla Casey**[1], **Eva Corey**[2], **Colm Morrissey**[2], **R. Mark Simpson**[3], and **Kathleen Kelly**[1,*]

[1]Laboratory of Genitourinary Cancer Pathogenesis, Center for Cancer Research, NCI, NIH, Bethesda, MD

[2]Department of Urology, University of Washington, Seattle, WA

[3]Laboratory of Cancer Biology and Genetics, Center for Cancer Research, NCI, NIH, Bethesda, MD

Abstract

Prostate cancer is characterized by a dependence upon androgen receptor (AR) signaling, and androgen deprivation therapy (ADT) is the accepted treatment for progressive prostate cancer. Although ADT is usually initially effective, acquired resistance, termed castrate resistant prostate cancer (CRPC) develops. *PTEN* and *TP53* are two of the most commonly deleted or mutated genes in prostate cancer, the compound loss of which is enriched in CRPC. To interrogate the metabolic alterations associated with survival following ADT, we used an orthotopic model of *Pten*/Tp53 null prostate cancer. Metabolite profiles and associated regulators were compared in tumors from androgen intact mice and in tumors surviving castration. AR inhibition led to changes in the levels of glycolysis and TCA cycle pathway intermediates. As anticipated for inhibitory reciprocal feedback between AR and PI3K/AKT signaling pathways, pAKT levels were increased in androgen deprived tumors. Elevated mitochondrial HK2 levels and enzyme activities also were observed in androgen-deprived tumors, consistent with pAKT dependent HK2 protein induction and mitochondrial association. Competitive inhibition of HK2 mitochondrial binding in prostate cancer cells led to decreased viability. These data argue for AKT-associated HK2-mediated metabolic reprogramming and mitochondrial association in PI3K driven prostate cancer as one survival mechanism downstream of AR inhibition.

[*]**Correspondence:** Kathleen Kelly, PhD; Building 37, Room 1068A, Bethesda, MD 20892; 301-435-4651; 301-435-4655 (FAX); kellyka@mail.nih.gov.

[#]Present address: Medimmune, Gaithersburg, MD

Conflict of interest:

The authors declare no conflict of interest.

Introduction

Prostate cancer is the second leading cause of cancer-related mortality in men[1]. Most cancer-related deaths are attributable to metastatic disease. Recurrent and metastatic prostate cancers are treated with androgen deprivation therapy[14, 49]. Castrate resistant prostate cancer, which almost always eventually develops following ADT, is often characterized by acquired mutations in the androgen receptor (AR) signaling pathway[17, 39]. The general lack of AR pathway mutations in primary prostate cancers and the existence of distinct AR pathway mutations within different metastases from a single individual imply that mutations giving rise to acquired resistance occur after metastatic spread[18, 39]. Thus, there appear to be genetic driver alterations in high risk primary prostate cancers that both promote progression and may govern the initial tumor survival to androgen deprivation[25]. The capability to tolerate/survive ADT independent of AR pathway mutations is hypothesized to be an early step in the evolution of some aggressive, AR-dependent CRPC's[12, 47, 52]. Outcomes for men with high risk primary prostate cancer or early metastatic disease may be improved by ADT in combination with agents targeting parallel pathways contributing to tumor proliferation and survival in low androgen conditions[49]. Here we have investigated metabolic reprogramming that occurs in aggressive prostate cancer cells that survive androgen deprivation.

Prostate cancer metabolism is an area of active inquiry with applications for metabolic imaging and biomarker diagnostics as well as for targeted therapies. Although there is a high degree of genetic and clinical heterogeneity among prostate cancers, common metabolic reprogramming properties observed in prostate cancers have been recognized. Normal prostate cells secrete large amounts of citrate into prostatic fluid, a property that blunts the Krebs cycle[11]. Prostate cancer cells decrease citrate secretion and reactivate the Krebs cycle, which influences the cellular redox state and metabolic flux through interdigitated pathways. Another early and common metabolic alteration in prostate cancer is an aberrant increase in de novo lipogenesis resulting from increased expression of key enzymes involved in fatty acid and cholesterol synthesis[51]. Recent evidence supports the concept that certain oncogenic drivers of prostate cancer influence distinct metabolic programs[36]. Integrative analyses of metabolomic signatures in combination with RNA and protein levels of metabolic enzymes have linked high activation of AKT1 in prostate cancer with changes to glycolysis and other glucose-related pathways[36]. By contrast, MYC overexpression combined with low AKT1 activation is characterized by dysregulated lipid metabolism. Thus, the glycolytic phenotype of prostate cancers, which is variable, probably reflects the heterogeneity of prostate cancer driver mutations[20].

An important pAKT effector is HK2, an enzyme that catalyzes the first committed step of glucose metabolism, facilitating all major pathways of glucose utilization. HK is required for tumor initiation and maintenance in several experimental models, including prostate cancer[35, 48]. HK2 is thought to be a major contributor to enhanced energy production as a result of mitochondrial localization which facilitates coupling glycolysis and oxidative phosphorylation[4, 26]. Also, metabolic flux analyses in HK2 deleted lung cancer cells have suggested that HK2 indirectly influences other important growth-related pathways including non-oxidative ribonucleotide synthesis and glutamine-dependent anapleurosis[35]. HK2 binds

and inhibits TORC1 to facilitate autophagy in response to glucose deprivation[37], potentially facilitating energetic homeostasis following stress. Finally, HK2 binding to mitochondria decreases apoptotic susceptibility by preventing mitochondrial death pathways[26].

In order to analyze metabolic patterns correlated with prostate cancer survival in an androgen deprived environment, we have used an orthotopic model of primary *Pten/Tp53* null mouse prostate cancer. The loss or mutation of *PTEN*, a negative regulator of the PI3K/AKT pathway, occurs in about 20% of primary prostate cancers and is enriched to about 40% in CRPC[7, 17, 39]. *PTEN* loss in clinical prostate cancer is associated with various properties of aggressive disease including increased future risk of biochemical recurrence[9, 30], as well as decreased time to metastasis[24] and increased prostate cancer specific mortality in high-risk cohorts[30, 42]. Prior work in mouse models has implicated *Pten* loss as a potential cause of tumor survival and growth following castration[15, 21, 33]. In parallel with *PTEN* mutations, *TP53* genomic modifications are significantly increased (from about 10 to 50%) in castrate resistant relative to primary prostate cancer[7, 17, 39]. Recently, in-depth sequencing of matched primary and metastatic prostate cancers has suggested that *TP53* mutations are drivers of metastatic potential in low-frequency subclones[19]. TP53 has pleiotropic effects on a variety of cellular functions including cell cycle progression, metabolism, genome stability, and stem cell differentiation[6, 23]. Compared to PB-CRE4 driven *Pten* null prostate cancer, the PB-CRE4;$Pten^{fl/fl}$;$Tp53^{fl/fl}$ prostate cancer model produces significantly faster growing tumors with increased histological heterogeneity, consistent with amplified numbers of luminal cancer stem/progenitor cells that have been demonstrated in this model[3, 28].

Analyzing the interacting systemic, microenvironmental, and tumor-dependent effects of castration on survival and metabolism requires in vivo models. Although in vitro studies analyzing metabolic pathways relative to AR pathway activation have been important for dissecting isolated regulatory mechanisms[29], in vitro models cannot faithfully replicate the complexities of ADT in vivo. Here, metabolomic as well as select enzymatic and expression analyses were determined for androgen intact tumors and for tumors surviving androgen deprivation. We present evidence that increased AKT activation, changed glucose metabolism, and HK2 activity associated with mitochondria are correlated with survival in an androgen-deprived environment.

Results

Androgen withdrawal leads to increased pAKT expression and the selection of castration-tolerant cell populations

We sought to investigate metabolic changes which occur in tumor cells surviving androgen withdrawal. The experimental scheme, which included two dosage arms, is shown in Figure 1A. Briefly, castrated mice were injected orthotopically with Clone 1 cells and implanted subcutaneously with either 5 or 12.5 mg slow release testosterone capsules at the time of surgery. At a time point when tumors were established, mice were randomized to have testosterone capsules either maintained (referred to as “androgen intact”) or removed (“androgen deprived”). Mice continued on study until tumor growth was advanced and became locally invasive leading to morbidity, usually as a result of urinary obstruction. The

average median survival for androgen intact mice from both cohorts was 8 weeks compared to 11.5 or 10 weeks for androgen deprived mice originally implanted with 5 or 12.5 mg capsules, respectively (the 5 mg cohort is shown in Figure 1B). Tumors were characterized for a variety of properties, including metabolic profiles, histology, and selected transcriptomic, proteomic, and enzymatic activities.

Histologically, tumors were composed of adenocarcinomas admixed with a minority basal/squamous component that was typically more well represented in androgen deprived tumors[28]. In the both 5 and 12.5 mg testosterone dosage cohorts, there was frequent lymphovascular invasion, with the lung being the most common site of distant metastasis, as described previously for Clone 1 cells[28]. Microarray analysis of androgen deprived as compared to intact tumors, demonstrated a loss of AR-dependent gene transcripts, as shown for *Msmb, Fkbp5*, and *Pbsn*, as well as an increase in genes such as *Wnt16*[44] and *Pcdhb11*[46], which have been associated with human prostate cancer survival in androgen deprived conditions (Figure 1C). Dual label IHC for pAKT and Ki67 was performed on tumor sections obtained from androgen intact and deprived animals and analyzed by automated quantification (Figure 1D). Tumor cells surviving castration were noticeably less proliferative with significantly increased pAKT levels. Increased pAKT levels are consistent with mutually-inhibitory AR-PI3K pathway cross-regulation described previously[8, 33]. pAKT expression levels correlated with dividing cells in androgen-intact tumors ($r = 0.59$). However, in androgen-deprived tumors, the correlation between $pAKT^+$ and $Ki67^+$ cells decreased ($r = 0.32$), reflecting the presence of a subpopulation with high pAKT and low Ki67 labeling (Figure 1D). These data suggest that high pAKT levels alone are not sufficient for proliferation in an androgen-deprived environment but may be associated with survival.

A metabolomics screen identified depletion of carbohydrates and glycogen stores, increased glycolysis, and changes to TCA cycle intermediates

To determine if androgen deprivation altered metabolic pathways in the generated tumors, we performed a broad spectrum metabolite profile screen on samples collected at necropsy (Figure 2). In addition to two cohorts of Clone 1 tumors, another previously characterized *Pten/Tp53* null androgen-sensitive luminal progenitor cell line (Plum-C)[2] was included as outlined in Figure 1A. More differences were observed between androgen deprived and intact Clone 1 tumors in the 12.5 as compared to the 5 mg testosterone cohorts. The most consistent changes in metabolism between intact and androgen deprived orthotopic tumors were decreases in monosaccharides that can be converted into glucose-6-phosphate for glycolysis. In androgen deprived compared to androgen intact animals, tumor fructose, mannitol, and sorbitol levels were decreased, while glycogen breakdown products were increased. The increase in monosaccharide and glycogen metabolism may be a result of depleted glucose, observed in the three androgen-withdrawal conditions. In addition, there was accumulation of the aerobic glycolysis metabolite lactate in Clone 1 (12.5mg) and Plum-C androgen depleted tumors.

For TCA cycle metabolites, there was a decrease in citrate levels in the androgen deprived as compared to the androgen intact tumors (Figure 2). However, despite this decrease in citrate, the first intermediate in the TCA cycle, later intermediates (fumarate and malate) increased

in the androgen deprived relative to the androgen intact tumors, consistent with replenishment of TCA cycle intermediates via anaplerosis, i.e. glutaminolysis to replenish α-ketoglutarate and aspartate conversion to oxaloacetate. Levels of aspartate and glutamate also were increased in the androgen deprived relative to intact tumors. We note that fatty acid and cholesterol levels were similar in androgen deprived and intact tumors (Supplemental Figure 1), suggesting either a lack of androgen regulation or a return to homeostasis at the time of harvest.

Our results have parallels with reported metabolome profiles for human prostate cancer. Interestingly, there are changes such as decreased fructose and glucose and/or increased lactate within subsets of aggressive prostate cancer that mirror the changes described here for androgen deprived tumors[22, 31, 36]. In addition, other pathways (Supplemental Figure 2) such as modified betaine-dimethylglycine-sarcosine metabolism and scylloinositol- myo-inositol metabolism[43, 45] demonstrate similar patterns between increasingly aggressive human prostate cancer and androgen deprived vs. intact *Pten/Tp53* null mouse tumors.

Androgen deprivation leads to increased levels of several genes involved in key energetic pathways related to carbohydrate metabolism

In order to determine if there were transcriptional differences associated with the metabolomic differences observed in androgen deprived tumors, we performed a focused metabolic gene expression analysis (Qiagen™) on tumors from the 12.5 mg testosterone arm. The expression of several genes in glycolysis, glycogen metabolism, TCA cycle, and pentose phosphate pathways were significantly increased in the androgen deprived relative to the intact tumors (Supplemental Figure 3). Interestingly, all of the significant changes in the metabolic pathways tested were in the direction of increased expression in androgen deprived tumors relative to androgen intact tumors.

Androgen deprivation leads to increased hexokinase enzyme activity

Next we analyzed whether changes to glucose metabolism following androgen deprivation were accompanied by changes in the activity of two key enzymes, hexokinase (HK) and pyruvate dehydrogenase. Frozen tumor samples were fractionated into soluble and particulate fractions. The soluble HK activity was approximately 35% greater in the androgen deprived tumors (Figure 3A). The particulate HK activity was approximately 3.4 fold greater in the androgen deprived tumors; although there was a high degree of variability among individual tumors. The activity of pyruvate dehydrogenase, the final enzyme in the pathway linking glycolysis and the TCA cycle, is shown in Figure 3A. There were no significant differences between the pyruvate dehydrogenase activities of the soluble or particulate fractions comparing androgen intact and deprived tumors.

To determine whether androgen deprivation resulted in autonomous effects on tumor cells with respect to increased hexokinase activity, we assayed Clone 1 cells, grown in vitro either with or without DHT for 24 hours. Cells were fractionated into cytoplasmic and mitochondrial compartments (Figure 3B). Cells incubated in the absence relative to the presence of DHT showed significant increases in HK activity in both fractions. Independent

of DHT treatment, the enzyme activity in the mitochondrial fraction was approximately 6–7 fold greater than the levels in the cytoplasmic compartment.

Hexokinase 2 protein levels increase following androgen deprivation in vivo and correlate with cellular proliferation

We sought to determine whether the increased enzymatic activity following androgen deprivation in Clone 1 tumors resulted from increased HK2 protein expression because pAKT/mTORC1 signaling positively regulates HK2 levels[16, 37, 48]. Androgen deprived prostate carcinomas in this model have a large degree of heterogeneity in cellular proliferation. Thus, we used dual color immunohistochemistry to perform semi-quantitative scoring of HK2 levels in both proliferating ($Ki67^+$) and non-proliferating ($Ki67^-$) adenocarcinoma cells. This dual color IHC staining, shown in Figure 4A and quantified in Figure 4B, demonstrated increased levels of HK2 in both proliferating and non-proliferating cells in androgen deprived tumors relative to the androgen intact tumors, consistent with increased pAKT in quiescent and proliferating cells. Interestingly, in both androgen intact and androgen deprived tumors, the mean per cell HK2 scores in proliferating cells were significantly higher than in non-proliferating cells (Figure 4B and Supplemental Figure 4). We also used automated quantification which confirmed a correlation between HK2 levels and proliferation and demonstrated a statistically significant increased slope (HK2 levels relative to $\%Ki67^+$) in androgen-deprived compared to androgen-intact tumors (Figure 4C). Taken together, our results suggest that androgen deprivation leads to increased HK2 levels throughout the tumor cell populations and that HK2 levels positively correlate with cell division. Because there is a subpopulation of $pAKT^+Ki67^-$ cells in androgen-deprived tumors (Figure 1D), this further suggests that pAKT levels alone do not determine HK2 levels but that additional factors also play a role. Finally, since HK2 RNA does not significantly increase in vivo following androgen deprivation (Supplemental Figure 3), this suggests that HK2 levels are post-transcriptionally controlled.

Androgen deprivation leads to increased mitochondrial associated HK2, which promotes survival

pAKT regulates the association of HK2 with mitochondria[26, 37]. To determine whether the large increase in HK2 activity in the particulate cellular fraction of androgen-deprived orthotopic tumors was consistent with mitochondrial associated-HK2, we performed dual labeling confocal microscopy on 4% PFA fixed paraffin embedded orthotopic tumors to co-localize HK2 and mitochondrial VDAC1, a component of the outer mitochondrial membrane and the binding site for HK2 (Figure 5A). This analysis revealed co-localization of HK2 and VDAC1, but not HK2 and nuclei, demonstrating the presence of mitochondrial HK2.

We next investigated the functional role of mito-HK2 in Clone 1 cells. As shown in Figure 3B, there is increased mitochondrial-associated HK activity in Clone 1 cells incubated in the absence compared to the presence of DHT in vitro, and the majority of this activity is associated with mitochondria. Similar to the in vivo results, androgen deprivation in vitro resulted in increased HK2 protein levels (Figure 5B).

To determine whether HK2 binding to mitochondria is necessary for optimal cell growth, we used a cell-permeable, competitive peptide inhibitor of HK2 mitochondrial binding[5] (Figure 5C). Following twelve hour incubations with two concentrations of the inhibitor peptide, we observed concentration-dependent decreases in cellular viability and relatively increased viability of the androgen-deprived compared to the androgen-intact cell cultures. These results imply that some level of HK2 association with mitochondria is necessary for optimal survival of Clone 1 cells. In addition, the graded response is consistent with higher total and mitochondrial levels of HK2 in androgen-deprived conditions, requiring higher peptide concentrations for equivalent reduction of mitochondrial HK2 association levels.

HK2 expression patterns in primary prostate cancer and CRPC

Prior studies demonstrated that HK2 levels increase in primary prostate cancer relative to normal prostate epithelia[48]. To extend these studies, we analyzed HK2 staining patterns in primary prostate cancer and in soft tissue and bone metastases from CRPC. As shown in Figure 6, our analysis using a scoring index which takes into account staining intensity and percentage of positive cells validates increased HK2 expression of prostate cancer compared to normal prostate. Interestingly, CRPC showed a large range in expression levels with the upper range being similar to primary prostate cancer and a portion of cases similar to or lower than normal prostate epithelia. We believe that the diversity of HK2 expression levels may reflect the fact that CRPC demonstrates considerable heterogeneity in underlying genomics, mechanisms of acquired resistance to androgen deprivation, and histological features[40, 41]. In contrast to the experimental studies performed here that involve early survival/growth responses to androgen deprivation, human CRPC usually evolves after extended selection leading to acquired resistance, sometimes to more than one treatment modality[14, 49].

Discussion

AR pathway inhibition has long been the treatment of choice for men with metastatic prostate cancer, but acquired resistance limits the long-term durability of such treatment[14, 49]. One path to acquired resistance hypothesizes the adaption to survival and growth in a subpopulation of cells despite low AR signaling, with subsequent AR pathway alteration and selection for rapid growth[12, 52]. Although much attention has been devoted to mechanisms of acquired resistance, it has been challenging to investigate the genetic and environmental factors that facilitate adaptation to the androgen deprived state prior to acquired resistance. Here we have investigated metabolic adaptation following androgen deprivation in a model of prostate cancer initiated by deletion of *Pten* and *Tp53*, mutations that are common in primary prostate cancer and are further selected in CRPC[17, 39].

We report here that androgen deprivation leads to changes in glucose metabolism observed as depletion of monosaccharide pools, increased lactate, and changes to TCA cycle intermediates of decreased citrate and increase fumarate and malate. We observed increased AKT activation as well as elevated HK2 protein expression and particulate hexokinase enzyme activity in tumors from androgen-deprived animals. By catalyzing the phosphorylation of glucose, HK2 promotes and sustains a concentration gradient that

facilitates glucose entry into cells, initiating glycolysis and glucose-linked pathways. Evidence exists for HK2 influencing both the magnitude and direction of glucose flux within cells[35]. Importantly, AKT-dependent HK2 mitochondrial association is a well-recognized mechanism of protecting mitochondria against stress[26, 37]. These data argue for one mechanism, which integrates metabolic reprogramming and cell survival as a consequence of linked AR inhibition and AKT pathway activation, leading to increased HK2 levels and mitochondrial association.

Given the importance of AR and PI3K/AKT signaling in clinically aggressive prostate cancer, experimental mouse models and human studies have evaluated cross-regulation of the AR and AKT signaling pathways in PTEN null prostate cancers[8, 33]. *PTEN* loss suppresses AR transcriptional output, and AR inhibition leads to AKT activation as a result of decreased *FKBP5* expression, which impairs the stability of the AKT phosphatase, PHLPP. Therefore, AR-dependent and AKT-dependent growth/survival signals regulate each other by reciprocal feedback, leading to an apparent coordinated support of survival. As shown in Figure 1, *Fkbp5* expression was decreased and pAKT expression was significantly increased in *Pten/Tp53* null tumor cells surviving ADT. Although a number of survival pathways downstream of AKT activation are known, the specific consequences of AKT activation in the context of AR inhibition have not been delineated. We suggest that increased HK2 levels and mitochondrial association observed following castration is a likely pathway for mediating both pAKT-associated metabolic reprogramming and survival signaling. Prior work has demonstrated mTORC1-dependent translational and TP53 dependent transcriptional regulation of constitutively elevated HK2 levels in PTEN/TP53 null prostate cancer models[48]. Here we have extended the analysis of HK2 regulation to clinically-relevant cell signaling and metabolic responses to androgen deprivation.

In addition to its role in metabolism, HK2 is well recognized as a protein that promotes cell survival. Cytosolic HK activity appears to be important in some systems for indirectly controlling the levels of reactive oxygen species (ROS) as a result of diverting glucose into the pentose phosphate pathway[35, 50]. Importantly for the castration model investigated here, AKT activation has been shown in various models to promote HK2-mitochondrial binding and protection[38]. Mitochondrial associated HKs exert protective effects to prevent mitochondrial death pathways. HKs antagonize the binding of apoptotic BCL2 family members at the mitochondrial outer membrane[27, 34]. In addition, mito-HK2 has a direct inhibitory effect upon the mitochondrial transition pore, the opening of which leads to mitochondrial rupture and necrotic death[10, 26]. Consistent with an important role for mitochondrial bound HK2, the prostate cancer cells used in this study lost viability proportionately to the displacement of HK2 from mitochondria mediated by a competitive mitochondrial binding HK2 peptide (Figure 5).

In summary, we have evaluated for one of the first times, the metabolic response of aggressive, orthotopically located prostate cancer cells to androgen deprivation. *Pten/Tp53* null cells surviving castration exhibited reduced AR dependent gene expression, increased pAKT levels, and altered glucose metabolism. Consistent with a known role in pAKT driven metabolic reprogramming and stress survival, our results show increased HK2 levels, enzyme activity and mitochondrial association in surviving tumor cells. Such knowledge

contributes to a fundamental understanding of prostate cancer physiology and informs the use of biomarkers and metabolic imaging for monitoring the ADT responses of prostate cancers with documented PI3K/AKT activation.

Materials and Methods

In vitro culture:

Clone 1 cells are a $KRT8^+AR^+$ clonal cell line derived from a prostate adenocarcinoma of *Pb-Cre4*$^+$;*Pten*$^{fl/fl}$;*P53*$^{fl/fl}$ mice[28]. Clone 1 cells were cultured in PrEGM (Lonza, MD) containing 5nM DHT, 5% FCS, and 5% 3T3 conditioned media. The derivation and characterization of the prostate cancer stem cell line, Plum-C, was previously described[2]. TAT-HK and TAT-Control peptides were purchased from Pepscan (custom-made, Pepscan). Viability was measured using MTS assays (Promega, WI). Detailed information for reagents is contained in Supplemental Table 1.

Animal Experiments:

All animal care was provided in accordance with the procedures outlined by the National Cancer Institute Guideline for the Care and Use of Laboratory Animals. To establish the orthotopic model, clone 1 cells were inoculated into the anterior prostate of 12 weeks old male nude mice through an abdominal incision. At the time of surgery mice were castrated and either implanted with a subcutaneous 5mg or a 12.5mg testosterone capsule. Mice implanted with 5 mg capsules had capsules either removed (n=9) or replenished (n=8) at week 7 post injection. Mice implanted with 12.5 mg capsules had capsules either removed (n=7) or remained intact (n=8) at week 4 before tumors were palpable. Sample size was recommended by Metabolon Inc. Mice were assigned to each group by cage randomization. Mice in both cohorts continued on study until signs of morbidity, usually due to urinary obstruction, were observed.

Immunohistochemistry:

Immunohistochemistry was performed as described previously[28]. Orthotopic tumors were removed and fixed with 4% paraformaldehyde for standard histological processing, sectioning and staining (Histoserve Inc., MD). IHC staining conditions were optimized for each antibody. Primary antibody concentrations used are as follows. Ki-67 (Abcam, 1/600), HK2 (Cell Signaling, 1/50), pAKT (Cell Signaling, 1/50), pAMPK (Cell Signaling, 1/100), VDAC1(Abcam, 1/100). For dual color IHC to Ki67/HK2 and Ki67/pAKT, a sequential staining protocol was used. Slides were first incubated with Ki67 for 1 hour, followed by the standard Vector ABC IHC protocol and detection with ImmPACT NovaRED. Slides were then washed in PBST. HK2 or pAKT antibodies were then applied and incubated overnight at 4C. A routine Vector ABC IHC protocol was used with DAB detection.

For manual scoring of per cell HK2 levels, images were captured at 20X, comprising the entire tumor area, using the Aperio™ system. Semi-quantitative cytoplasmic HK2 labeling was assessed in a manner blinded to sample identification in 100 $Ki67^+$ cells followed by 100 $Ki67^-$ cells. Each cell was scored for labeling intensity as follows: 0:negative, 1:minimal/mild; 2:moderate; 3:strong.

Ariol™ scanning/analysis platform was used for automated detection. The slides were scanned at 20X. The entire tumor region was divided into equal 150 μm^2 regions of interest (ROI). The following features were counted for each ROI using the color and size parameters: number of $Ki67^+$ nuclei, number of $Ki67^-$ hematoxylin counter stained nuclei, and % area of DAB stain ($HK2^+$ or $pAKT^+$) cytoplasm. For each ROI the % nuclei positive for Ki67 and the % area positive for DAB stain were plotted and analyzed using Graph Pad Prizm™.

Prostate TMAs containing primary tumors (UWTMA48) or soft tissue and bone metastases (UWTMA22) were acquired from the University of Washington with the Prostate Cancer Donor Rapid Autopsy Program[32]. Tumor cell HK2 levels were scored with the following grading scheme: Scores for each array core were the sum of intensity score and % cell positive score as follows: intensity score (0:negative, 1:weak, 2:moderate, 3:strong, 4:very strong) and % cells positive score (0:less than 10%, 1:11–25%, 2:26–50%, 3:51–75%, and 4:76–100%). Each score represents the average of two cores per sample.

Reverse Transcriptase PCR:

Glucose Metabolism RT-PCR array (Qiagen, Frederick, MD) was used to analyze the expression of 84 genes involved in glucose/TCA/glycogen/gluconeogenesis/and pentose phosphate pathway metabolism. Reverse transcription was performed with the SuperScript III kit (Invitrogen, Carlsbad). For all primer pairs, the thermocycler was run for 40 cycles with a 10 minutes initial 95°C incubation, followed by 15 seconds 95°C melting, 30 seconds 55°C annealing, and 30 seconds 72°C extension.

Western Blotting:

Mitochondria and cytoplasmic fractions were isolated with a mitochondria isolation kit (ThermoScientific). HK2 (Cell Signaling, 1:1000) and VDAC1 (Abcam, 1/100) specific antibodies were used at the indicated concentrations.

Metabolomics:

Metabolites from flash frozen tumor samples were quantified at Metabolon Inc. (Durham, NC) using a non-targeted metabolomics gas and liquid chromatography coupled to mass spectrometry (GC/MS and LC/MS^2) platforms[13]. Briefly, samples were processed on a Hamilton MLStar (Hamilton Company, Salt Lake City, UT) robotics system using a proprietary series of organic and aqueous extractions in order to remove the protein fraction and to achieve maximum small molecules recovery. Each of the sample extract was divided into two fractions for analysis by LC and GC.

Enzyme Activity Assays:

The enzymatic activities of hexokinase and pyruvate dehydrogenase were measured using the Hexokinase enzyme assay kit (E-111) and the Pyruvate dehydrogenase assay kit (E-109) from Biomedical Research Service and Clinical Application (Buffalo, NY).

RNA expression analysis:

Microarrays (GeneChip Gene 1.0 ST Arrays, Affymetrix) were performed by the Genomics Technology Laboratory Core at the Frederick National Laboratory using total RNAs extracted from Clone 1 tumors (5 mg cohort) from either androgen intact (n=5) or deprived (n=5) mice. Gene expression differences were validated by qPCR for individual tumors.

Statistical Methods:

For metabolomic analysis, Welch's t-tests and/or Wilcoxon's rank sum tests were used for pair-wise comparisons. ANOVA was used for other statistical designs. Random forest analyses were used for classification. Statistical analyses are performed with the program "R." For IHC, enzyme activity and other in vitro experiments, data were analyzed using Prizm software (GraphPad Software, Inc.) by one way ANOVA followed by Bonferroni post-test when comparing more than two groups, or by t-test when two groups were compared. Results are expressed as mean ± SD. $P < 0.05$ was considered significant.

Supplementary Material

Refer to Web version on PubMed Central for supplementary material.

Acknowledgments:

We appreciated the patients and their families who participated in the Prostate Cancer Donor Program. We thank the investigators Drs. Robert Vessella, Celestia Higano, Bruce Montgomery, Evan Yu, Peter Nelson, Paul Lange, Martine Roudier, and Lawrence True for their contributions to the University of Washington Medical Center Prostate Cancer Donor Rapid Autopsy Program. This research was supported by the Intramural Research Program, Center for Cancer Research, NCI, and by the Pacific Northwest Prostate Cancer SPORE (P50CA97186), the PO1 NIH grant (PO1CA085859) and the Richard M. LUCAS Foundation.

References

1. American Cancer Society (2015). Cancer Facts and Figures 2015. http://www.cancer.org/acs/groups/content/@editorial/documents/document/acspc-044552.
2. Abou-Kheir W, Hynes PG, Martin P, Yin JJ, Liu YN, Seng V et al. Self-renewing Pten−/− TP53−/− protospheres produce metastatic adenocarcinoma cell lines with multipotent progenitor activity. PloS one 2011; 6: e26112. [PubMed: 22022528]
3. Agarwal S, Hynes PG, Tillman HS, Lake R, Abou-Kheir WG, Fang L et al. Identification of Different Classes of Luminal Progenitor Cells within Prostate Tumors. Cell reports 2015.
4. Arora KK, Pedersen PL. Functional significance of mitochondrial bound hexokinase in tumor cell metabolism. Evidence for preferential phosphorylation of glucose by intramitochondrially generated ATP. The Journal of biological chemistry 1988; 263: 17422–17428. [PubMed: 3182854]
5. Arzoine L, Zilberberg N, Ben-Romano R, Shoshan-Barmatz V. Voltage-dependent anion channel 1-based peptides interact with hexokinase to prevent its anti-apoptotic activity. The Journal of biological chemistry 2009; 284: 3946–3955. [PubMed: 19049977]
6. Bonizzi G, Cicalese A, Insinga A, Pelicci PG. The emerging role of p53 in stem cells. Trends Mol Med 2011; 18: 6–12. [PubMed: 21907001]
7. Cancer Genome Atlas Research Network. Electronic address scmo, Cancer Genome Atlas Research N. The Molecular Taxonomy of Primary Prostate Cancer. Cell 2015; 163: 1011–1025. [PubMed: 26544944]
8. Carver BS, Chapinski C, Wongvipat J, Hieronymus H, Chen Y, Chandarlapaty S et al. Reciprocal feedback regulation of PI3K and androgen receptor signaling in PTEN-deficient prostate cancer. Cancer cell 2011; 19: 575–586. [PubMed: 21575859]

9. Chaux A, Peskoe SB, Gonzalez-Roibon N, Schultz L, Albadine R, Hicks J et al. Loss of PTEN expression is associated with increased risk of recurrence after prostatectomy for clinically localized prostate cancer. Modern pathology: an official journal of the United States and Canadian Academy of Pathology, Inc 2012; 25: 1543–1549.
10. Chiara F, Castellaro D, Marin O, Petronilli V, Brusilow WS, Juhaszova M et al. Hexokinase II detachment from mitochondria triggers apoptosis through the permeability transition pore independent of voltage-dependent anion channels. PloS one 2008; 3: e1852. [PubMed: 18350175]
11. Costello LC, Franklin RB. The clinical relevance of the metabolism of prostate cancer; zinc and tumor suppression: connecting the dots. Molecular cancer 2006; 5: 17. [PubMed: 16700911]
12. Craft N, Chhor C, Tran C, Belldegrun A, DeKernion J, Witte ON et al. Evidence for clonal outgrowth of androgen-independent prostate cancer cells from androgen-dependent tumors through a two-step process. Cancer research 1999; 59: 5030–5036. [PubMed: 10519419]
13. Evans AM, DeHaven CD, Barrett T, Mitchell M, Milgram E. Integrated, nontargeted ultrahigh performance liquid chromatography/electrospray ionization tandem mass spectrometry platform for the identification and relative quantification of the small-molecule complement of biological systems. Analytical chemistry 2009; 81: 6656–6667. [PubMed: 19624122]
14. Ferraldeschi R, Welti J, Luo J, Attard G, de Bono JS. Targeting the androgen receptor pathway in castration-resistant prostate cancer: progresses and prospects. Oncogene 2014.
15. Gao H, Ouyang X, Banach-Petrosky WA, Shen MM, Abate-Shen C. Emergence of androgen independence at early stages of prostate cancer progression in Nkx3.1; Pten mice. Cancer research 2006; 66: 7929–7933. [PubMed: 16912166]
16. Gottlob K, Majewski N, Kennedy S, Kandel E, Robey RB, Hay N. Inhibition of early apoptotic events by Akt/PKB is dependent on the first committed step of glycolysis and mitochondrial hexokinase. Genes & development 2001; 15: 1406–1418. [PubMed: 11390360]
17. Grasso CS, Wu YM, Robinson DR, Cao X, Dhanasekaran SM, Khan AP et al. The mutational landscape of lethal castration-resistant prostate cancer. Nature 2012; 487: 239–243. [PubMed: 22722839]
18. Gundem G, Van Loo P, Kremeyer B, Alexandrov LB, Tubio JM, Papaemmanuil E et al. The evolutionary history of lethal metastatic prostate cancer. Nature 2015; 520: 353–357. [PubMed: 25830880]
19. Hong MK, Macintyre G, Wedge DC, Van Loo P, Patel K, Lunke S et al. Tracking the origins and drivers of subclonal metastatic expansion in prostate cancer. Nature communications 2015; 6: 6605.
20. Jadvar H Molecular imaging of prostate cancer with PET. Journal of nuclear medicine: official publication, Society of Nuclear Medicine 2013; 54: 1685–1688.
21. Jiao J, Wang S, Qiao R, Vivanco I, Watson PA, Sawyers CL et al. Murine cell lines derived from Pten null prostate cancer show the critical role of PTEN in hormone refractory prostate cancer development. Cancer research 2007; 67: 6083–6091. [PubMed: 17616663]
22. Kami K, Fujimori T, Sato H, Sato M, Yamamoto H, Ohashi Y et al. Metabolomic profiling of lung and prostate tumor tissues by capillary electrophoresis time-of-flight mass spectrometry. Metabolomics: Official journal of the Metabolomic Society 2013; 9: 444–453. [PubMed: 23543897]
23. Kruiswijk F, Labuschagne CF, Vousden KH. p53 in survival, death and metabolic health: a lifeguard with a licence to kill. Nature reviews Molecular cell biology 2015; 16: 393–405. [PubMed: 26122615]
24. Lotan TL, Gurel B, Sutcliffe S, Esopi D, Liu W, Xu J et al. PTEN protein loss by immunostaining: analytic validation and prognostic indicator for a high risk surgical cohort of prostate cancer patients. Clinical cancer research: an official journal of the American Association for Cancer Research 2011; 17: 6563–6573. [PubMed: 21878536]
25. Lunardi A, Ala U, Epping MT, Salmena L, Clohessy JG, Webster KA et al. A co-clinical approach identifies mechanisms and potential therapies for androgen deprivation resistance in prostate cancer. Nature genetics 2013; 45: 747–755. [PubMed: 23727860]

26. Majewski N, Nogueira V, Bhaskar P, Coy PE, Skeen JE, Gottlob K et al. Hexokinase-mitochondria interaction mediated by Akt is required to inhibit apoptosis in the presence or absence of Bax and Bak. Molecular cell 2004; 16: 819–830. [PubMed: 15574336]
27. Majewski N, Nogueira V, Robey RB, Hay N. Akt inhibits apoptosis downstream of BID cleavage via a glucose-dependent mechanism involving mitochondrial hexokinases. Molecular and cellular biology 2004; 24: 730–740. [PubMed: 14701745]
28. Martin P, Liu YN, Pierce R, Abou-Kheir W, Casey O, Seng V et al. Prostate epithelial Pten/TP53 loss leads to transformation of multipotential progenitors and epithelial to mesenchymal transition. Am J Pathol 2011; 179: 422–435. [PubMed: 21703421]
29. Massie CE, Lynch A, Ramos-Montoya A, Boren J, Stark R, Fazli L et al. The androgen receptor fuels prostate cancer by regulating central metabolism and biosynthesis. The EMBO journal 2011; 30: 2719–2733. [PubMed: 21602788]
30. McCall P, Witton CJ, Grimsley S, Nielsen KV, Edwards J. Is PTEN loss associated with clinical outcome measures in human prostate cancer? British journal of cancer 2008; 99: 1296–1301. [PubMed: 18854827]
31. McDunn JE, Li Z, Adam KP, Neri BP, Wolfert RL, Milburn MV et al. Metabolomic signatures of aggressive prostate cancer. The Prostate 2013; 73: 1547–1560. [PubMed: 23824564]
32. Morrissey C, Roudier MP, Dowell A, True LD, Ketchanji M, Welty C et al. Effects of androgen deprivation therapy and bisphosphonate treatment on bone in patients with metastatic castration-resistant prostate cancer: results from the University of Washington Rapid Autopsy Series. Journal of bone and mineral research: the official journal of the American Society for Bone and Mineral Research 2013; 28: 333–340.
33. Mulholland DJ, Tran LM, Li Y, Cai H, Morim A, Wang S et al. Cell autonomous role of PTEN in regulating castration-resistant prostate cancer growth. Cancer cell 2011; 19: 792–804. [PubMed: 21620777]
34. Pastorino JG, Shulga N, Hoek JB. Mitochondrial binding of hexokinase II inhibits Bax-induced cytochrome c release and apoptosis. The Journal of biological chemistry 2002; 277: 7610–7618. [PubMed: 11751859]
35. Patra KC, Wang Q, Bhaskar PT, Miller L, Wang Z, Wheaton W et al. Hexokinase 2 is required for tumor initiation and maintenance and its systemic deletion is therapeutic in mouse models of cancer. Cancer cell 2013; 24: 213–228. [PubMed: 23911236]
36. Priolo C, Pyne S, Rose J, Regan ER, Zadra G, Photopoulos C et al. AKT1 and MYC induce distinctive metabolic fingerprints in human prostate cancer. Cancer research 2014; 74: 7198–7204. [PubMed: 25322691]
37. Roberts DJ, Miyamoto S. Hexokinase II integrates energy metabolism and cellular protection: Akting on mitochondria and TORCing to autophagy. Cell death and differentiation 2015; 22: 364. [PubMed: 25578149]
38. Robey RB, Hay N. Mitochondrial hexokinases, novel mediators of the antiapoptotic effects of growth factors and Akt. Oncogene 2006; 25: 4683–4696. [PubMed: 16892082]
39. Robinson D, Van Allen EM, Wu YM, Schultz N, Lonigro RJ, Mosquera JM et al. Integrative clinical genomics of advanced prostate cancer. Cell 2015; 161: 1215–1228. [PubMed: 26000489]
40. Roudier MP, True LD, Higano CS, Vesselle H, Ellis W, Lange P et al. Phenotypic heterogeneity of end-stage prostate carcinoma metastatic to bone. Hum Pathol 2003; 34: 646–653. [PubMed: 12874759]
41. Shah RB, Mehra R, Chinnaiyan AM, Shen R, Ghosh D, Zhou M et al. Androgen-independent prostate cancer is a heterogeneous group of diseases: lessons from a rapid autopsy program. Cancer research 2004; 64: 9209–9216. [PubMed: 15604294]
42. Sircar K, Yoshimoto M, Monzon FA, Koumakpayi IH, Katz RL, Khanna A et al. PTEN genomic deletion is associated with p-Akt and AR signalling in poorer outcome, hormone refractory prostate cancer. The Journal of pathology 2009; 218: 505–513. [PubMed: 19402094]
43. Stenman K, Stattin P, Stenlund H, Riklund K, Grobner G, Bergh A. H HRMAS NMR Derived Biomarkers Related to Tumor Grade, Tumor Cell Fraction, and Cell Proliferation in Prostate Tissue Samples. Biomarker insights 2011; 6: 39–47. [PubMed: 21499438]

44. Sun Y, Campisi J, Higano C, Beer TM, Porter P, Coleman I et al. Treatment-induced damage to the tumor microenvironment promotes prostate cancer therapy resistance through WNT16B. Nature medicine 2012; 18: 1359–1368.
45. Swanson MG, Vigneron DB, Tabatabai ZL, Males RG, Schmitt L, Carroll PR et al. Proton HR-MAS spectroscopy and quantitative pathologic analysis of MRI/3D-MRSI-targeted postsurgical prostate tissues. Magnetic resonance in medicine 2003; 50: 944–954. [PubMed: 14587005]
46. Terry S, Queires L, Gil-Diez-de-Medina S, Chen MW, de la Taille A, Allory Y et al. Protocadherin-PC promotes androgen-independent prostate cancer cell growth. The Prostate 2006; 66: 1100–1113. [PubMed: 16637074]
47. Toivanen R, Frydenberg M, Murphy D, Pedersen J, Ryan A, Pook D et al. A preclinical xenograft model identifies castration-tolerant cancer-repopulating cells in localized prostate tumors. Sci Transl Med 2013; 5: 187ra171.
48. Wang L, Xiong H, Wu F, Zhang Y, Wang J, Zhao L et al. Hexokinase 2-mediated Warburg effect is required for PTEN- and p53-deficiency-driven prostate cancer growth. Cell reports 2014; 8: 1461–1474. [PubMed: 25176644]
49. Watson PA, Arora VK, Sawyers CL. Emerging mechanisms of resistance to androgen receptor inhibitors in prostate cancer. Nature reviews Cancer 2015; 15: 701–711. [PubMed: 26563462]
50. Wu R, Wyatt E, Chawla K, Tran M, Ghanefar M, Laakso M et al. Hexokinase II knockdown results in exaggerated cardiac hypertrophy via increased ROS production. EMBO molecular medicine 2012; 4: 633–646. [PubMed: 22517678]
51. Zadra G, Photopoulos C, Loda M. The fat side of prostate cancer. Biochimica et biophysica acta 2013; 1831: 1518–1532. [PubMed: 23562839]
52. Zong Y, Goldstein AS. Adaptation or selection--mechanisms of castration-resistant prostate cancer. Nat Rev Urol 2013; 10: 90–98. [PubMed: 23247694]

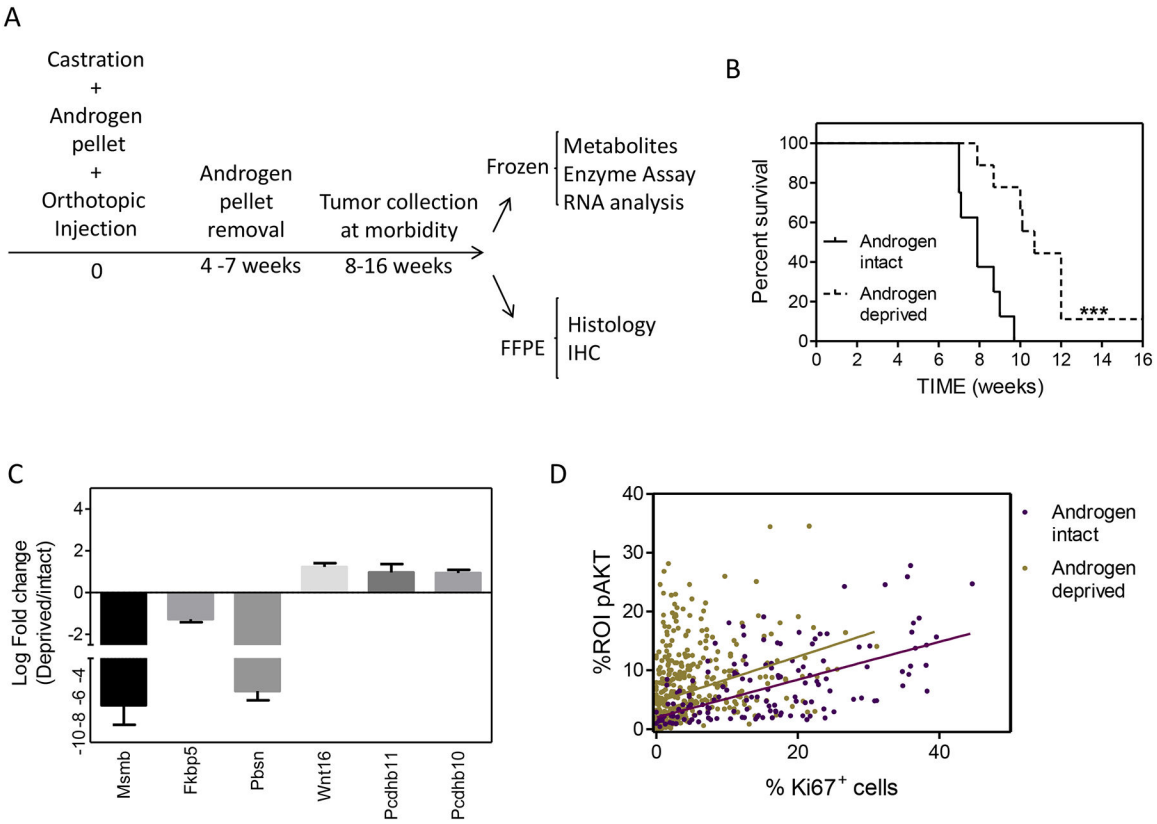

Figure 1.

Characterizing the response to androgen deprivation in an orthotopic mouse model. A) Experimental ADT time line and tissue procurement. B) Survival rate of mice in androgen intact and deprived (5 mg cohort) groups. Data were analyzed by log-rank test. ***p<0.001. C) Representative genes regulated in Clone 1 tumors by androgen deprivation. D) Correlation analysis of primary tumor sections in androgen intact and androgen deprived groups. Sections were dual stained for Ki67 and pAKT and scored using an automated platform. n=5 mice / group. The Pearson *r* values are 0.59 and 0.32 for androgen intact and androgen deprived, respectively.

		testosterone		
		Clone1		Plum-C
pathway	Biochemical names	5mg	12.5mg	5mg
Fructose, mannose, galactose, starch, and sucrose metabolism	fructose	0.02	0.00	0.00
	6'-sialyllactose	0.99	1.37	1.17
	maltose	1.43	1.73	0.45
	mannitol	0.09	0.06	0.05
	mannose	0.34	0.25	0.09
	sorbitol	0.06	0.03	0.04
	maltotriose	1.98	2.86	1.00
	maltotetraose	2.25	7.93	**0.52**
Glycolysis, gluconeogenesis, pyruvate metabolism	1,5-anhydroglucitol (1,5-AG)	0.96	**1.59**	0.61
	glycerate	0.27	0.07	0.10
	glucose-6-phosphate (G6P)	1.94	1.40	0.55
	glucose	0.50	0.48	0.09
	Isobar: fructose 1,6-diphosphate, glucose 1,6-diphosphate	0.99	**0.50**	0.71
	phosphoglycerate (2 or 3)	0.76	**0.50**	0.54
	lactate	0.85	**1.28**	1.71
	glucuronate	1.86	1.17	2.29
Krebs cycle	citrate	0.77	0.35	0.60
	cis-aconitate	0.75	0.28	0.60
	succinate	0.84	1.29	**1.44**
	succinylcarnitine	0.73	1.25	**1.51**
	fumarate	1.06	1.51	1.16
	malate	1.02	1.33	1.12
Oxidative phosphorylation	acetylphosphate	0.90	1.29	0.92
	phosphate	1.06	1.37	1.11
	pyrophosphate (PPi)	1.07	**1.35**	1.13
Alanine and aspartate metabolism	alanine	1.16	1.61	1.89
	beta-alanine	1.07	**1.56**	0.50
	N-acetylalanine	**1.46**	1.85	1.45
	N-acetyl-beta-alanine	1.66	2.03	**1.30**
	aspartate	**1.37**	1.78	1.02
	N-acetylaspartate (NAA)	8.89	2.71	1.24
	3-ureidopropionate	3.41	**2.05**	4.65
Glutamate metabolism	glutamate	1.02	1.39	1.59
	glutamate, gamma-methyl ester	1.42	1.58	**1.27**
	glutamine	1.16	1.30	1.04
	gamma-aminobutyrate (GABA)	0.43	0.12	0.11
	N-acetylglutamate	2.83	2.07	2.15

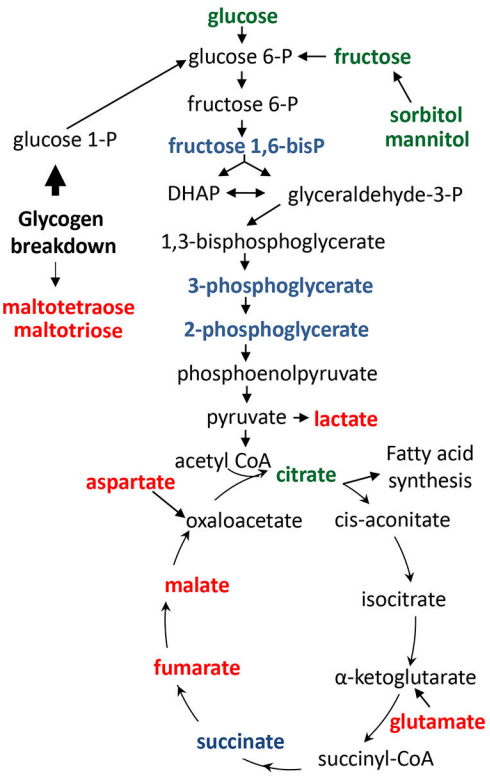

Figure 2.

Selected metabolite quantifications for *Pten*$^{fl/fl}$;*TP53*$^{fl/fl}$ orthotopic prostate carcinomas growing in androgen intact or deprived male mice. Left) Heat map depicting metabolic changes in androgen deprived relative to intact orthotopic tumors for several key energetic pathways. Values indicate ratio of androgen deprived vs androgen intact groups. Significance differences ($p<0.05$) are indicated by colored cells. Green cells indicate a ratio <1; red cells indicate a ratio > 1; bold blue numbers indicate narrowly missed cutoff for significance; $0.05< p <0.10$. Numbers of tumors analyzed for Clone 1 (5mg testosterone), Clone 1 (12.5mg testosterone), and Plum-C cohorts: intact- 7, 7, and 5 respectively, and for deprived- 6, 6, and 5, respectively. Right) Integrated model of metabolic changes in glycolysis and the tricarboxylic acid (TCA) cycle. Red indicates enhanced metabolite levels; green indicates reduced metabolite levels, and blue indicates trends narrowly missing significance as observed for at least one of the three cohorts.

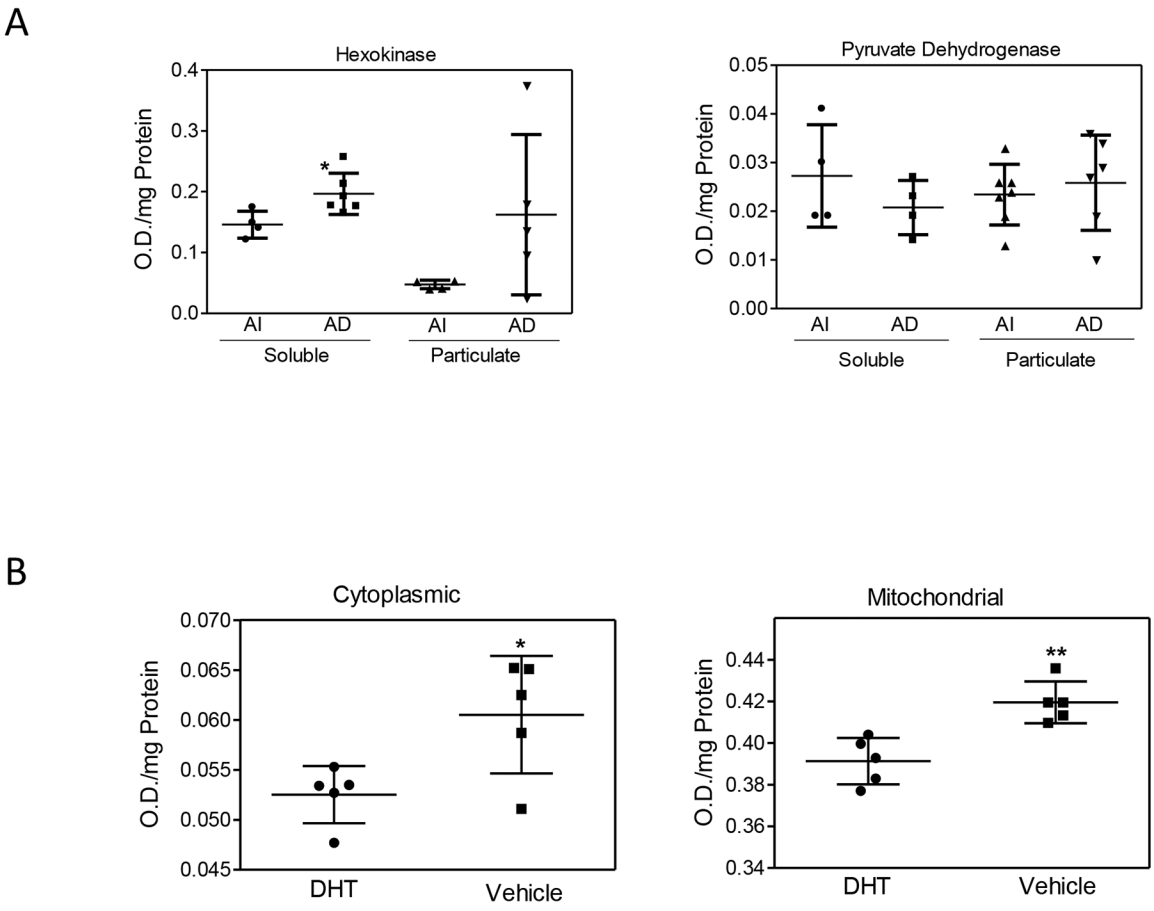

Figure 3.

Quantification of hexokinase activities in vivo and in vitro. A) Hexokinase (left panel) and Pyruvate Dehydrogenase (right panel) activities assayed from soluble and particulate fractions of androgen intact (AI) (n=4) and androgen deprived (AD) (n=7) tumors. B) Hexokinase enzyme activity in cytoplasmic (left panel) and mitochondrial (right panel) fractions measured from Clone1 cells treated with or without 5nM DHT for 24 hours. Data were analyzed with t-test. *p<0.05, **p<0.01

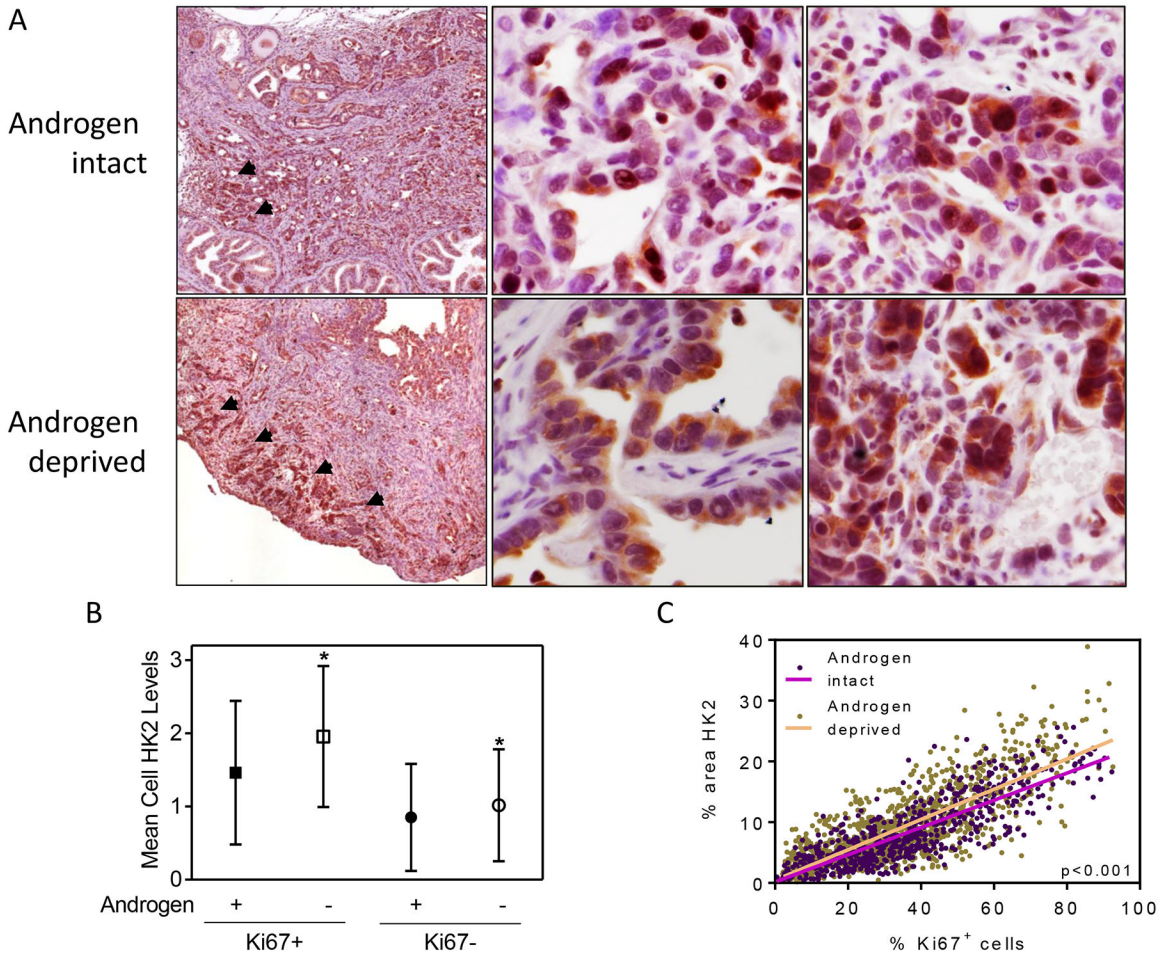

Figure 4.

Quantification of HK2 expression relative to tumor cell proliferation. A) Representative dual color immunohistochemistry demonstrates HK2 (brown) and Ki67 (red) expression in androgen intact (upper panels) and androgen deprived (lower panels) tumors. The left panels are low power images from Aperio scanner, the middle panels are high HK2 expressing regions, and the right panels are lower HK2 expressing regions. B) Semi-quantitative score of cytoplasmic HK2 in Ki67 positive and negative cells comparing androgen intact (n=7) and deprived (n=6) tumor sections. For each orthotopic tumor 100 $Ki67^+$ cells and 100 $Ki67^-$ cells were randomly chosen and scored semi-quantitatively for cytoplasmic HK2 levels (0=negative, 1=minimal/mild, 2=moderate, 3=strong). Data were analyzed by ANOVA followed by Bonferroni post test. *$p<0.05$. C) Correlation analysis of HK2 and Ki67 staining cells in primary tumor sections as determined using the automated Ariol™ scanning/analysis platform (n=7 for androgen intact and n=6 for deprived groups). Each dot represents a 150μm^2 region of interest (ROI). Light purple and orange lines represent linear regression. $p<0.001$

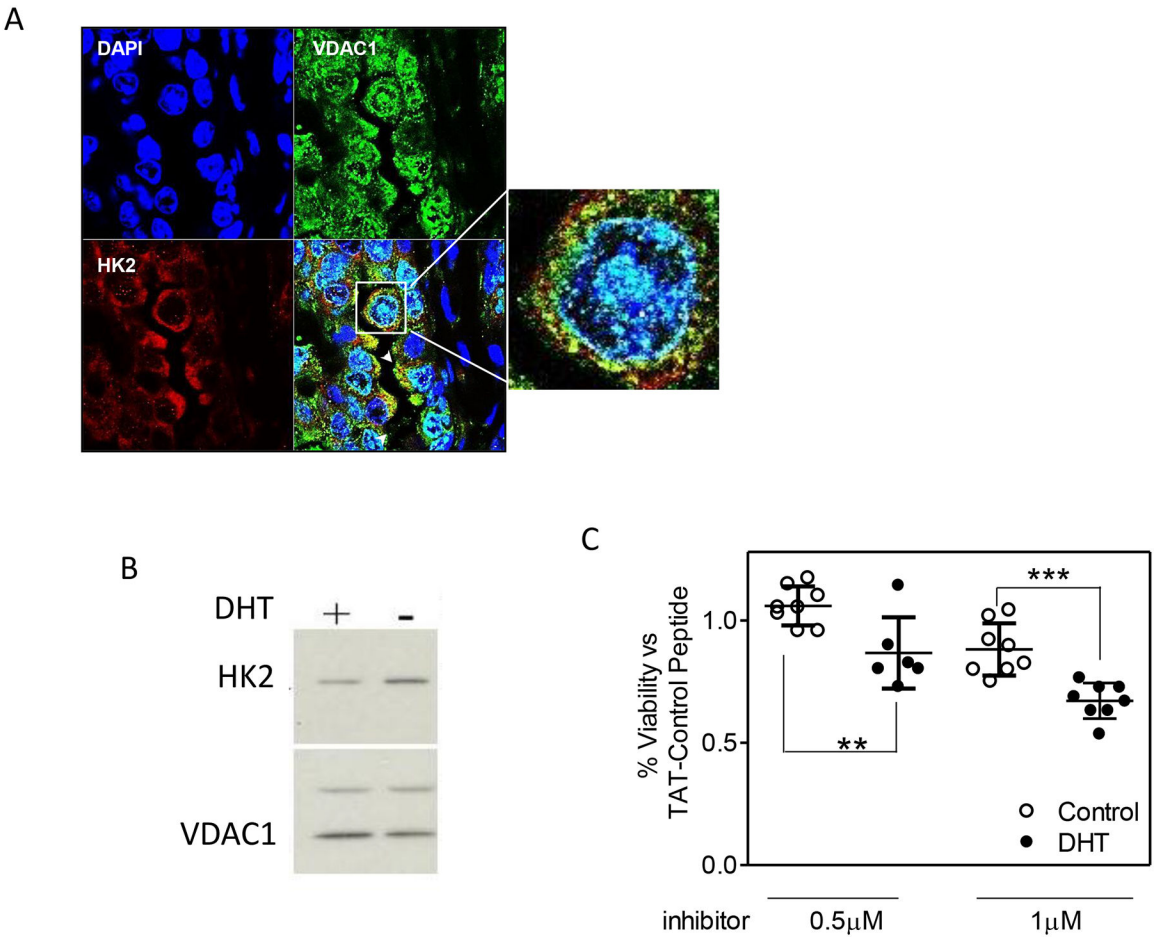

Figure 5.

Mitochondria HK2 expression in androgen intact and androgen deprived conditions. A) Representative confocal microscopy image of mitochondrial localization of HK2 (red), VDAC1(green), and DAPI-stained nuclei (blue) in a section of androgen-deprived Clone 1 tumor. B) Western blot analysis of HK2 expression in Clone 1 cells treated with or without 5 nM DHT for 24 hours. VDAC1 was used as a mitochondria loading control. C) Viability assay for Clone 1 cells grown with or without DHT for 24 hours and with the indicated concentrations of TAT-HK2 or TAT-Control peptides. Data were analyzed by t test. **p<0.01, ***p<0.001.

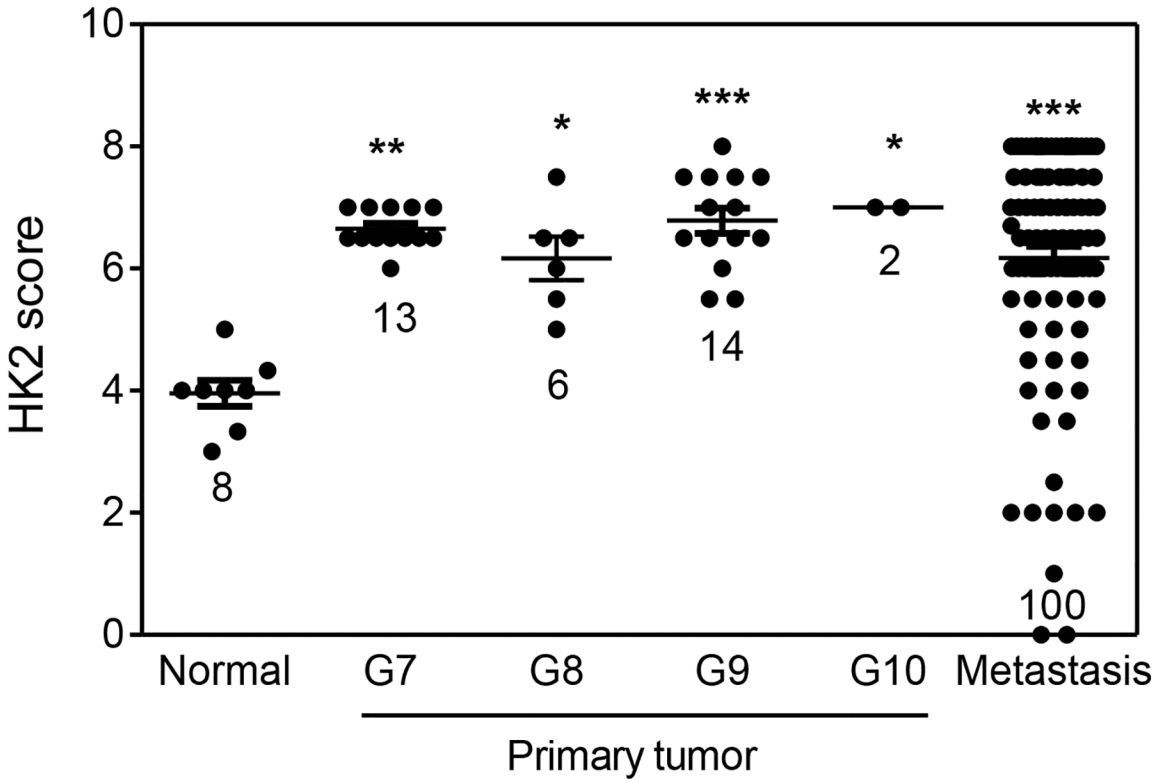

Figure 6.

HK2 expression in human TMA samples including normal prostate, primary prostate tumors with Gleason scores ranging from 7 to 10, and metastatic prostate tumors. Each symbols represents one core. Data were analyzed by ANOVA followed by Bonferroni post test. *: $p<0.05$, **: $p<0.01$, ***: $p<0.001$ vs normal.